Syracuse University
SURFACE

Physics | College of Arts and Sciences

11-23-2010

Search for Rare and Forbidden Decays of Charm and Charmed-Strange Mesons to Final States h+- e-+ e+

Raymond Mountain
Syracuse University, rjmounta@syr.edu

Marina Artuso
Syracuse University, artuso@physics.syr.edu

S. Blusk
Syracuse University

T. Skwarnicki
Syracuse University

Follow this and additional works at: http://surface.syr.edu/phy

Part of the Physics Commons

Repository Citation
Mountain, Raymond; Artuso, Marina; Blusk, S.; and Skwarnicki, T., "Search for Rare and Forbidden Decays of Charm and Charmed-Strange Mesons to Final States h+- e-+ e+" (2010). *Physics.* Paper 349.
http://surface.syr.edu/phy/349

This Article is brought to you for free and open access by the College of Arts and Sciences at SURFACE. It has been accepted for inclusion in Physics by an authorized administrator of SURFACE. For more information, please contact surface@syr.edu.

CLNS 10/2068
CLEO 10-05

Search for rare and forbidden decays of charm and charmed-strange mesons to final states $h^{\pm}e^{\mp}e^{+}$

P. Rubin,[1] N. Lowrey,[2] S. Mehrabyan,[2] M. Selen,[2] J. Wiss,[2] J. Libby,[3] M. Kornicer,[4] R. E. Mitchell,[4] M. R. Shepherd,[4] C. M. Tarbert,[4] D. Besson,[5] T. K. Pedlar,[6] J. Xavier,[6] D. Cronin-Hennessy,[7] J. Hietala,[7] P. Zweber,[7] S. Dobbs,[8] Z. Metreveli,[8] K. K. Seth,[8] A. Tomaradze,[8] T. Xiao,[8] S. Brisbane,[9] L. Martin,[9] A. Powell,[9] P. Spradlin,[9] G. Wilkinson,[9] H. Mendez,[10] J. Y. Ge,[11] D. H. Miller,[11] I. P. J. Shipsey,[11] B. Xin,[11] G. S. Adams,[12] D. Hu,[12] B. Moziak,[12] J. Napolitano,[12] K. M. Ecklund,[13] J. Insler,[14] H. Muramatsu,[14] C. S. Park,[14] L. J. Pearson,[14] E. H. Thorndike,[14] F. Yang,[14] S. Ricciardi,[15] C. Thomas,[9,15] M. Artuso,[16] S. Blusk,[16] R. Mountain,[16] T. Skwarnicki,[16] S. Stone,[16] J. C. Wang,[16] L. M. Zhang,[16] G. Bonvicini,[17] D. Cinabro,[17] A. Lincoln,[17] M. J. Smith,[17] P. Zhou,[17] J. Zhu,[17] P. Naik,[18] J. Rademacker,[18] D. M. Asner,[19,*] K. W. Edwards,[19] K. Randrianarivony,[19] G. Tatishvili,[19,*] R. A. Briere,[20] H. Vogel,[20] P. U. E. Onyisi,[21] J. L. Rosner,[21] J. P. Alexander,[22] D. G. Cassel,[22] S. Das,[22] R. Ehrlich,[22] L. Fields,[22] L. Gibbons,[22] S. W. Gray,[22] D. L. Hartill,[22] B. K. Heltsley,[22] D. L. Kreinick,[22] V. E. Kuznetsov,[22] J. R. Patterson,[22] D. Peterson,[22] D. Riley,[22] A. Ryd,[22] A. J. Sadoff,[22] X. Shi,[22] W. M. Sun,[22] and J. Yelton[23]

(CLEO Collaboration)

[1] *George Mason University, Fairfax, Virginia 22030, USA*
[2] *University of Illinois, Urbana-Champaign, Illinois 61801, USA*
[3] *Indian Institute of Technology Madras, Chennai, Tamil Nadu 600036, India*
[4] *Indiana University, Bloomington, Indiana 47405, USA*
[5] *University of Kansas, Lawrence, Kansas 66045, USA*
[6] *Luther College, Decorah, Iowa 52101, USA*
[7] *University of Minnesota, Minneapolis, Minnesota 55455, USA*
[8] *Northwestern University, Evanston, Illinois 60208, USA*
[9] *University of Oxford, Oxford OX1 3RH, United Kingdom*
[10] *University of Puerto Rico, Mayaguez, Puerto Rico 00681*
[11] *Purdue University, West Lafayette, Indiana 47907, USA*
[12] *Rensselaer Polytechnic Institute, Troy, New York 12180, USA*
[13] *Rice University, Houston, Texas 77005, USA*
[14] *University of Rochester, Rochester, New York 14627, USA*
[15] *STFC Rutherford Appleton Laboratory, Chilton, Didcot, Oxfordshire, OX11 0QX, United Kingdom*
[16] *Syracuse University, Syracuse, New York 13244, USA*
[17] *Wayne State University, Detroit, Michigan 48202, USA*
[18] *University of Bristol, Bristol BS8 1TL, United Kingdom*
[19] *Carleton University, Ottawa, Ontario, Canada K1S 5B6*
[20] *Carnegie Mellon University, Pittsburgh, Pennsylvania 15213, USA*
[21] *University of Chicago, Chicago, Illinois 60637, USA*
[22] *Cornell University, Ithaca, New York 14853, USA*
[23] *University of Florida, Gainesville, Florida 32611, USA*

(Dated: September 9, 2010)

arXiv:1009.1606v3 [hep-ex] 23 Nov 2010

Abstract

We have searched for flavor-changing neutral current decays and lepton-number-violating decays of D^+ and D_s^+ mesons to final states of the form $h^\pm e^\mp e^+$, where h is either π or K. We use the complete samples of CLEO-c open-charm data, corresponding to integrated luminosities of 818 pb^{-1} at the center-of-mass energy $E_{\rm CM} = 3.774$ GeV containing 2.4×10^6 D^+D^- pairs and 602 pb^{-1} at $E_{\rm CM} = 4.170$ GeV containing 0.6×10^6 $D_s^{*\pm}D_s^\mp$ pairs. No signal is observed in any channel, and we obtain 90% confidence level upper limits on branching fractions $\mathcal{B}(D^+ \to \pi^+e^+e^-) < 5.9\times10^{-6}$, $\mathcal{B}(D^+ \to \pi^-e^+e^+) < 1.1\times10^{-6}$, $\mathcal{B}(D^+ \to K^+e^+e^-) < 3.0\times10^{-6}$, $\mathcal{B}(D^+ \to K^-e^+e^+) < 3.5\times10^{-6}$, $\mathcal{B}(D_s^+ \to \pi^+e^+e^-) < 2.2\times10^{-5}$, $\mathcal{B}(D_s^+ \to \pi^-e^+e^+) < 1.8\times10^{-5}$, $\mathcal{B}(D_s^+ \to K^+e^+e^-) < 5.2\times10^{-5}$, and $\mathcal{B}(D_s^+ \to K^-e^+e^+) < 1.7\times10^{-5}$.

* Present address: Pacific Northwest National Laboratory, Richland, WA 99352

I. INTRODUCTION

As an extension of our previously reported [1] search for rare and forbidden decays of the D^+ charm meson, $D^+ \to h^\pm e^\mp e^+$, we report an analysis using CLEO-c's full open-charm data sample for D^+, and also a search for $D_s^+ \to h^\pm e^\mp e^+$ with CLEO-c's full D_s^+ data sample. Here, h is either π or K, and charge-conjugate modes are implicit throughout this article. These decays probe flavor-changing neutral currents (FCNC), in $D^+ \to \pi^+ e^+ e^-$ and $D_s^+ \to K^+ e^+ e^-$, and lepton number violations (LNV), in $D^+ \to h^- e^+ e^+$ and $D_s^+ \to h^- e^+ e^+$. These decays are either highly suppressed or forbidden in the standard model (SM), but can be significantly enhanced by some non-SM physics scenarios [2–7]. Standard model short-distance FCNC decays are expected to be of order 10^{-10} to 10^{-9} [3, 5], but long-distance vector-pole induced decays of D^+ or $D_s^+ \to h^+ V^0 \to h^+ e^+ e^-$ (where V^0 is an intermediate vector meson ρ^0, ω, or ϕ) are expected to be of order 10^{-6} to 10^{-5} [3, 5]. To observe an enhancement in FCNC due to non-SM physics, we need to search for dielectron mass regions away from the vector poles. Measuring long-distance induced decay itself might be helpful to understand the long-distance dynamics in the b sector, such as inclusive $b \to s\gamma$ decay or exclusive $B \to \rho\gamma$ and $B \to K^*\gamma$ decays related to extracting Cabibbo-Kobayashi-Maskawa matrix elements $|V_{t(d,s)}|$. On the other hand, observation of LNV ($\Delta L = 2$) decays could be an indication of a Majorana nature of neutrinos [6, 7].

We have used two sets of open-charm data samples collected by the CLEO-c detector in e^+e^- collisions provided by the Cornell Electron Storage Ring (CESR). The integrated luminosities are 818 pb^{-1} at the center-of-mass energy $E_{\rm CM} = 3.774$ GeV near the peak of the $\psi(3770)$ resonance which decays to $D\bar{D}$ pairs, and 602 pb^{-1} at $E_{\rm CM} = 4.170$ GeV near the peak of $D_s^{*\pm} D_s^\mp$ pair production. The 3.774 GeV data set contains 2.4×10^6 D^+D^- pairs and is used to study $D^+ \to h^\pm e^\mp e^+$ decays. The 4.170 GeV data set contains 0.6×10^6 $D_s^{*\pm} D_s^\mp$ pairs, and is used to study $D_s^+ \to h^\pm e^\mp e^+$ decays.

The remainder of this article is organized as follows. The CLEO-c detector is described in Sec. II. Event selection criteria are described in Sec. III. Features of background processes, our suppression strategy, and signal sensitivity are discussed in Sec. IV. Results are presented as plots and tables in Sec. V. Systematic uncertainties associated with the branching fractions and their upper limits are discussed in Sec. VI. Finally, a summary of our results with systematic uncertainties is provided in Sec. VII.

II. THE CLEO-c DETECTOR

The CLEO-c detector [8–11] is a general-purpose solenoidal detector equipped with four concentric components: a six-layer vertex drift chamber, a 47-layer main drift chamber, a ring-imaging Cherenkov (RICH) detector, and a cesium iodide electromagnetic calorimeter, all operating inside a 1 Tesla magnetic field provided by a superconducting solenoidal magnet. The detector provides acceptance of 93% of the full 4π solid angle for both charged particles and photons. The main drift chamber provides specific-ionization (dE/dx) measurements that discriminate between charged pions and kaons. The RICH detector covers approximately 80% of 4π and provides additional separation of pions and kaons at momentum above 700 MeV. Hadron identification efficiencies are approximately 95% with misidentification rates of a few percent [12]. Electron identification is based on a likelihood variable that combines the information from the RICH detector, dE/dx, and the ratio of electromagnetic shower energy to track momentum (E/p). Typical electron identification

efficiency is well over 90% on average with the pion fake rate less than 0.1% and the kaon fake rate less than a percent [13, 14].

A GEANT-based [15] Monte Carlo (MC) simulation is used to study efficiencies of signal and background events. Physics events are generated by EVTGEN [16], tuned with improved knowledge of charm decays, and final-state radiation (FSR) is modeled by PHOTOS [17]. Nonresonant FCNC and LNV signal events are generated according to phase space.

III. EVENT SELECTION

Signal candidates are formed from sets of well-measured drift chamber tracks consistent with coming from the nominal interaction point. Charged pions and kaons are identified from the tracks with momentum greater than 50 MeV and with $|\cos\theta| < 0.93$, where θ is the angle between the track and the beam axis. Electron candidates are required to be above 200 MeV with $|\cos\theta| < 0.90$ to ensure that E/p is well measured.

At $E_{\rm CM} = 3.774$ GeV, for each signal candidate of the form $D^+ \to h^\pm e^\mp e^+$ (where h is either π or K), two kinematic variables are computed to define a signal region: the energy difference $\Delta E = E_{D^+} - E_{\rm beam}$ and the beam-constrained mass difference $\Delta M_{\rm bc} = [E^2_{\rm beam} - \mathbf{p}^2_{D^+}]^{1/2} - m_{D^+}$, where $(E_{D^+}, \mathbf{p}_{D^+})$ is the four-momentum of the signal D^+ candidate, $E_{\rm beam}$ is the beam energy, and m_{D^+} is the nominal [18] mass of the D^+ meson. To improve the resolution of the kinematic variables, we recover bremsstrahlung photon showers within 100 mrad of the direction of the electron candidates. We define a signal box for further analysis as $(\Delta E, \Delta M_{\rm bc}) = (\pm 20\,{\rm MeV}, \pm 5\,{\rm MeV})$, which corresponds to about 3-standard deviations of the kinematic variables. Because the expected contribution from the resonant decay $\mathcal{B}(D^+ \to \phi\pi^+ \to \pi^+e^+e^-) \sim \mathcal{O}(10^{-6})$ is within our sensitivity, we further subdivide $D^+ \to \pi^+e^+e^-$ candidates into two channels: resonant $D^+ \to \phi(e^+e^-)\pi^+$ and nonresonant $D^+ \to \pi^+e^+e^-$ for the FCNC search. If the dielectron invariant mass M_{ee} of the signal candidate is within ± 20 MeV of the nominal [18] mass of the ϕ meson, we treat it as a resonant $D^+ \to \phi(e^+e^-)\pi^+$ candidate and exclude it from the $D^+ \to \pi^+e^+e^-$ candidates.

Similarly, at $E_{\rm CM} = 4.170$ GeV, for each signal candidate of the form $D_s^+ \to h^\pm e^\mp e^+$, the following two variables are computed to define a signal region: the mass difference $\Delta M = M_{D_s^+} - m_{D_s^+}$ and the recoil mass (against the signal candidate) difference $\Delta M_{\rm recoil}(D_s^+) = [(E_0 - E_{D_s^+})^2 - (\mathbf{p}_0 - \mathbf{p}_{D_s^+})^2]^{1/2} - m_{D_s^{*+}}$, where $M_{D_s^+}$ is the invariant mass of the signal candidate, $m_{D_s^+}$ is the nominal [18] mass of the D_s^+, $(E_0, \mathbf{p}_0)$ is the total four-momentum of the e^+e^- beam taking the finite beam crossing angle into account, $(E_{D_s^+}, \mathbf{p}_{D_s^+})$ is the four-momentum of the signal candidate with $E_{D_s^+} = [m^2_{D_s^+} + \mathbf{p}^2_{D_s^+}]^{1/2}$, and $m_{D_s^{*+}}$ is the nominal [18] mass of the D_s^{*+}. The same bremsstrahlung recovery is performed and the $D_s^+ \to \pi^+e^+e^-$ channel is subdivided into resonant $\phi(e^+e^-)\pi^+$ and nonresonant channels. The signal box is defined as $(\Delta M, \Delta M_{\rm recoil}(D_s^+)) = (\pm 20\,{\rm MeV}, \pm 55\,{\rm MeV})$ for further analysis. The broad recoil mass window ± 55 MeV is required to allow both primary and secondary (from $D_s^{*+} \to D_s^+\gamma$ or $D_s^{*+} \to D_s^+\pi^0$) D_s^+ candidates to be selected.

IV. ANALYSIS

Backgrounds are dominantly from events with real electrons, particularly from D semileptonic decays. The majority of combinatorial background events are from double charm semileptonic decays, typically 4 or less charged particles in the event with large missing

energy due to the missing neutrinos. Hadronic decays involving γ-conversion and π^0 (η, ω) Dalitz decay, or accompanied by another charm semileptonic decay, can mimic the $h^{\pm}e^{\mp}e^{+}$ signal, as well. Because of the low probability of hadrons being misidentified as electrons [13], background from $D\bar{D}$ decays to 3-body charged-particle hadronic decays (such as $K^-\pi^+\pi^+$, $\pi^-\pi^+\pi^+$, $K^0_S K^+$, $K^+K^-\pi^+$) are negligible after two electrons are identified, and they do not peak at the signal region due to the wrong mass assignments for the hadrons misidentified as electrons. That is, $D\bar{D}$ backgrounds are predominantly associated with the semileptonic decays and non-$D\bar{D}$ ($q\bar{q}$ continuum, τ-pair, radiative return, or QED events) backgrounds are associated with the γ-conversion and Dalitz decays. All of these backgrounds are nonpeaking or peak away from the signal regions.

Our background suppression criteria tuning procedure for $D^+ \to h^{\pm}e^{\mp}e^{+}$ channels is detailed in our previous article [1]. We have used the same background rejection criteria with the four kinematic variables to reject the above-mentioned backgrounds in D^+ channels and revised the criteria to accommodate the D_s^+ channels. The other side total energy $E_{\rm other}$ is the sum of energies of all particles other than those making up the signal candidate. We use this variable to reject events associated with semileptonic decays, mainly for double charm semileptonic decays, in which the visible other side energy would be small due to the undetectable missing neutrinos. We reject candidates if $E_{\rm other} < 1.0$ GeV for $D^+ \to \pi^+e^+e^-$, $E_{\rm other} < 1.3$ GeV for $D^+ \to K^+e^+e^-$, $E_{\rm other} < 1.4$ GeV for $D_s^+ \to \pi^+e^+e^-$, and $E_{\rm other} < 1.7$ GeV for $D_s^+ \to K^+e^+e^-$. For the LNV modes, we reject candidates if the number of tracks in the event is 4 or fewer and $E_{\rm other} < 0.5$ GeV. Semileptonic events involving $K^0_S \to \pi^+\pi^-$ in the final state can mimic the signal in $\pi^+e^+e^-$ channels. We have used the invariant mass $M_{\pi^+\pi^-}$ to veto these events. We veto the candidate when the charged pion in the signal candidate combined with any other unused oppositely charged track satisfies $|M_{\pi^+\pi^-} - m_{K^0_S}| < 5$ MeV, where $m_{K^0_S}$ is the nominal [18] mass of the K^0_S. Real electrons from γ-conversion and Dalitz decays are suppressed by using the dielectron invariant mass squared q^2 computed from the signal electron positron pair, or $q^2_{\rm other}$ computed using one signal side electron (positron) combined with any oppositely charged unused track. We veto candidates if $q^2 < 0.01$ GeV^2 or $q^2_{\rm other} < 0.0025$ GeV^2. For D_s^+, we have required the solo photon from D_s^{*+} decays to $D_s^+\gamma$ to be explicitly reconstructed to further suppress underlying nonstrange-charmed meson backgrounds at $E_{\rm CM} = 4.170$ GeV, by requiring the recoil mass of the signal candidate plus solo photon $M_{\rm recoil}(D_s^+ + \gamma)$ to be within ± 30 MeV of the nominal [18] D_s^+ mass. Regardless of whether the signal D_s^+ candidate is the primary or secondary D_s^+, for the decay $e^+e^- \to D_s^{*\pm}D_s^{\mp} \to (D_s^{\pm}\gamma)D_s^{\mp}$, the mass of the system recoiling against the D_s^+ plus γ should peak at the D_s^+ mass.

The analysis was done in a blind fashion. Before we opened the signal box, all above-mentioned criteria were optimized using MC events with a sensitivity variable which is defined as the average upper limit one would get from an ensemble of experiments with the expected background and no signal,

$$\mathcal{S} = \frac{\sum_{N_{\rm obs}=0}^{\infty} \mathcal{C}(N_{\rm obs}|N_{\rm exp})\mathcal{P}(N_{\rm obs}|N_{\rm exp})}{N\epsilon}, \tag{1}$$

where $N_{\rm exp}$ is the expected number of background events, $N_{\rm obs}$ is the observed number of events, $\mathcal{C}$ is the 90% confidence coefficient upper limit on the signal, $\mathcal{P}$ is the Poisson probability, N is the number of D^+ or D_s^+, and ϵ is the signal efficiency. In addition to the signal MC samples, four types of background MC samples are utilized to optimize the background suppression criteria: 20 times the data sample for open-charm ($D\bar{D}$, $D^*\bar{D}$,

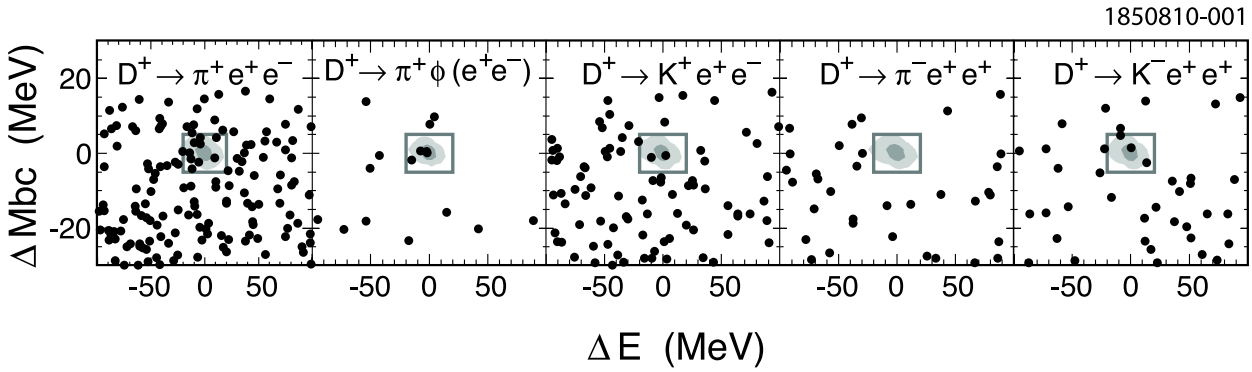

FIG. 1. Scatterplots of $\Delta M_{\rm bc}$ vs ΔE. The two contours for each mode enclose regions determined with signal MC simulation to contain 50% and 85% of signal events, respectively. The signal region, defined by $(\Delta E, \Delta M_{\rm bc}) = (\pm 20\,{\rm MeV}, \pm 5\,{\rm MeV})$, is shown as a box.

$D^*\bar{D}^*$, $D^*\bar{D}\pi$ $D_s^+D_s^-$, and $D_s^{*+}D_s^-$), 5 times the data sample of noncharm *uds* continuum ($q\bar{q}$), τ-pair, and radiative return to the $\psi(2S)$. To normalize background MC events to match the expected number of the data events, we have used integrated luminosity and cross sections for each process. For $D^+ \to h^\pm e^\mp e^+$ events at $E_{\rm CM} = 3774$ MeV, we have used $\sigma_{D^+D^-} = 2.91$ nb [12], $\sigma_{D^0\bar{D}^0} = 3.66$ nb [12], $\sigma_{q\bar{q}} = 13.9$ nb [19], $\sigma_{\tau^+\tau^-} = 3.0$ nb [1], and radiative return to the $\psi(2S)$ $\sigma_{\rm RR} = 3.4$ nb [20]. For $D_s^+ \to h^\pm e^\mp e^+$ events at $E_{\rm CM} = 4170$ MeV, we have used $\sigma_{D_s^{*\pm}D_s^\mp} = 0.916$ nb [21] (and used other open-charm cross sections from the same reference), $\sigma_{q\bar{q}} = 11.4$ nb [19], $\sigma_{\tau^+\tau^-} = 3.6$ nb, and radiative return to the $\psi(2S)$ $\sigma_{\rm RR} = 0.50$ nb [20]. We have found that the agreements between data and MC simulated events are excellent in various kinematic variables used in the background suppression, giving us confidence in our optimization procedure using our MC samples. Possible systematic uncertainties due to the data and MC differences are assessed in Sec. VI.

V. RESULTS

Scatterplots of ΔE vs $\Delta M_{\rm bc}$ and $\Delta M(D_s^+)$ vs $\Delta M_{\rm recoil}(D_s^+)$ for signal candidates with all background suppressions applied are shown in Figs. 1 and 2. Except for the $\phi(e^+e^-)\pi^+$ channels, we find no evidence of signals, and we calculate 90% confidence level upper limits (UL) on the branching fractions based on *Poisson processes with background* [22] (e.g. Section 28.6.4 *Poisson processes with background* therein) as summarized in Table I:

$$\mathrm{UL} = \frac{\mathcal{C}(N_{\rm obs}|N_{\rm exp})}{N\epsilon}. \tag{2}$$

For D^+ and $D_s^+ \to \phi(e^+e^-)\pi^+$ channels, we find weak evidence of signals with significance 3.5 for the D^+ and 1.8 for the D_s^+, so both branching fractions and upper limits are shown in Table I.

[1] With the lowest-order QED calculation, $\sigma(e^+e^- \to \tau^+\tau^-) = 2\pi\alpha^2\beta(3-\beta^2)/(3s)$, where $\beta = (1 - 4m_\tau^2/s)^{1/2}$ is the τ velocity.

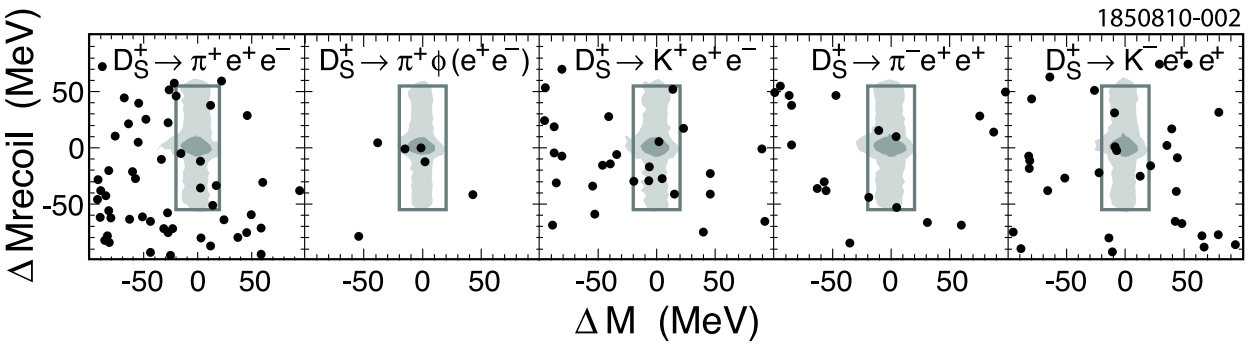

FIG. 2. Scatterplots of $\Delta M_{\rm recoil}$ vs ΔM. The two contours for each mode enclose regions determined with signal MC simulation to contain 40% and 85% of signal events, respectively. The signal region, defined by $(\Delta M, \Delta M_{\rm recoil}) = (\pm 20\,{\rm MeV}, \pm 55\,{\rm MeV})$, is shown as a box.

TABLE I. Upper limits on branching fractions of D^+ and $D_s^+ \to h^\pm e^\mp e^+$ at the 90% confidence level for a Poisson process [22], where N is the number of D^+ (or D_s^+) produced in our data, ϵ is the signal efficiency, $N_{\rm exp}$ is the number of expected background, $N_{\rm obs}$ is the number of signal candidates, $\mathcal{C}(N_{\rm obs}|N_{\rm exp})$ is the 90% confidence coefficient upper limit on the observed events given the expected background, and $\mathcal{B}$ is the branching fraction or upper limit of the branching fraction at 90% confidence level. We increase the upper limits to account for systematic uncertainties by decreasing the efficiency, the number of D^+ (or D_s^+), and the expected number of background each by 1 standard deviation. For the D^+ and $D_s^+ \to \phi(e^+e^-)\pi^+$ channels, we have shown both branching fractions and upper limits.

Channel	N	ϵ (%)	$N_{\rm exp}$	$N_{\rm obs}$	$\mathcal{C}(N_{\rm obs}\|N_{\rm exp})$	$\mathcal{B}$
$D^+ \to \pi^+ e^+ e^-$	4.76×10^6	33.9	5.7	9	9.3	$< 5.9 \times 10^{-6}$
$D^+ \to \pi^- e^+ e^+$	4.76×10^6	43.5	1.3	0	2.3	$< 1.1 \times 10^{-6}$
$D^+ \to K^+ e^+ e^-$	4.76×10^6	23.1	4.9	2	3.2	$< 3.0 \times 10^{-6}$
$D^+ \to K^- e^+ e^+$	4.76×10^6	35.3	1.2	3	5.8	$< 3.5 \times 10^{-6}$
$D^+ \to \pi^+ \phi(e^+e^-)$	4.76×10^6	46.2	0.3	4		$(1.7^{+1.4}_{-0.9} \pm 0.1) \times 10^{-6}$
					7.9	$< 3.7 \times 10^{-6}$
$D_s^+ \to \pi^+ e^+ e^-$	1.10×10^6	24.3	6.7	6	5.6	$< 2.2 \times 10^{-5}$
$D_s^+ \to \pi^- e^+ e^+$	1.10×10^6	33.4	2.2	4	6.2	$< 1.8 \times 10^{-5}$
$D_s^+ \to K^+ e^+ e^-$	1.10×10^6	17.3	3.0	7	9.3	$< 5.2 \times 10^{-5}$
$D_s^+ \to K^- e^+ e^+$	1.10×10^6	27.7	4.1	4	5.0	$< 1.7 \times 10^{-5}$
$D_s^+ \to \pi^+ \phi(e^+e^-)$	1.10×10^6	33.9	0.7	3		$(0.6^{+0.8}_{-0.4} \pm 0.1) \times 10^{-5}$
					6.2	$< 1.8 \times 10^{-5}$

VI. SYSTEMATIC UNCERTAINTIES

Possible sources of systematic uncertainty in our measurements are summarized in Table II. Uncertainties associated with upper limits are classified into three categories: uncertainties due to the normalization (the numbers of D^+ and D_s^+), the signal efficiency, and the number of expected background events.

Uncertainty in the number of D^+ (D_s^+) is estimated by adding contributions from uncer-

TABLE II. Summary of systematic uncertainties in D^+ and $D_s^+ \to h^\pm e^\mp e^+$ decays. Uncertainties associated with the branching fraction can be classified as three categories: uncertainties due to the normalization (the numbers of D^+ or D_s^+), the signal efficiency, and the number of background events. The columns labeled $\pi^+\phi$ refer to candidates with $\phi \to e^+e^-$ decays.

	D^+					D_s^+				
Source	$\pi^+e^+e^-$	$\pi^+\phi$	$\pi^-e^+e^+$	$K^+e^+e^-$	$K^-e^+e^+$	$\pi^+e^+e^-$	$\pi^+\phi$	$\pi^-e^+e^+$	$K^+e^+e^-$	$K^-e^+e^+$
Normalization	2.2%	2.2%	2.2%	2.2%	2.2%	5.6%	5.6%	5.6%	5.6%	5.6%
Tracking	0.9%	0.9%	0.9%	1.1%	1.1%	0.9%	0.9%	0.9%	1.1%	1.1%
PID	2.0%	2.0%	2.0%	2.0%	2.0%	2.0%	2.0%	2.0%	2.0%	2.0%
FSR	1.0%	1.0%	1.0%	1.0%	1.0%	1.0%	1.0%	1.0%	1.0%	1.0%
Background suppression	5.0%	4.2%	1.5%	9.4%	1.5%	5.2%	4.5%	2.1%	9.0%	2.2%
MC statistics	0.6%	0.6%	0.5%	0.8%	0.6%	0.8%	0.6%	0.6%	1.0%	0.7%
Efficiency total	5.6%	4.9%	2.9%	9.8%	3.0%	5.8%	5.1%	3.3%	9.3%	3.4%
Number of background	12%	68%	20%	12%	25%	12%	26%	16%	15%	11%

tainties in integrated luminosity [12] 1.0% and the production cross section [12] 2.0% (5.5% for D_s^+ [21]) in quadrature. We assign relative uncertainties of 2.2% to the number of D^+ and of 5.6% to the number of D_s^+.

There are several sources which can contribute to uncertainty in the signal efficiency estimation, as listed in Table II. By adding contributions from tracking [12], particle identification (PID) [12, 13], FSR [13, 14], background suppression, and MC statistics in quadrature we found total uncertainties in the signal efficiency for each channel range from 3% to 10%.

We use the number of background events estimated by the MC simulation rather than using the sidebands in data. The MC samples, being 5-20 times larger, have higher precision. We have evaluated possible systematic bias caused by the use of MC events rather than the data sideband by using alternative background shapes, and by comparing the MC predicted number to that interpolated from the data sideband. We found no indication of systematic bias; all deviations are adequately explained as statistical fluctuations due to the data statistics. We conclude that our MC events reproduce the features of the data backgrounds well. We took the statistical uncertainty in the MC simulated number of backgrounds as the systematic uncertainty in the expected number of background, as summarized in Table II.

VII. SUMMARY

With the complete samples of CLEO-c open-charm data, corresponding to integrated luminosities of 818 pb^{-1} at $E_{\rm CM} = 3.774$ GeV containing 2.4×10^6 D^+D^- pairs and 602 pb^{-1} at $E_{\rm CM} = 4.170$ GeV containing 0.6×10^6 $D_s^{*\pm}D_s^\mp$ pairs, we have searched for rare (FCNC) and forbidden (LNV) decays of D^+ and D_s^+ mesons of the form $h^\pm e^\mp e^+$, where $h^\pm$ is either a charged pion or a charged kaon. We found no evidence of signals and set upper limits on branching fractions at the 90% confidence level as summarized in Table I. Systematic uncertainties in the signal efficiency, the number of D^+ (or D_s^+) events, and the expected number of background events are incorporated by decreasing the numbers used for those quantities by 1 standard deviation of the systematic uncertainty on those quantities. These results are the most stringent limits on FCNC and LNV for the D^+ and $D_s^+ \to h^\pm e^\mp e^+$ decays to date and the limits in the dielectron channels are comparable to those in the dimuon channels [18], but are still a few orders of magnitude larger than the SM expectation [3, 5] in FCNC decays. This leaves some room for possible enhancement [2–5] in both FCNC and LNV decays induced by non-SM physics. We have separately measured branching fractions

of the resonant decays $D^+ \to \pi^+\phi \to \pi^+e^+e^-$ and $D_s^+ \to \pi^+\phi \to \pi^+e^+e^-$ due to their large expected contributions to $\pi^+e^+e^-$ channels. The significance of our measured branching fractions is poor at 3.5 standard deviations for D^+ and 1.8 standard deviations for D_s^+, so we have also included upper limits in Table I. Our measured branching fractions of these decays are consistent with the products of known world average [18] branching fractions, $\mathcal{B}(D^+ \to \phi\pi^+ \to e^+e^-\pi^+) = \mathcal{B}(D^+ \to \phi\pi^+) \times \mathcal{B}(\phi \to e^+e^-) = [(6.2 \pm 0.7) \times 10^{-3}] \times [(2.97 \pm 0.04) \times 10^{-4}] = (1.8 \pm 0.2) \times 10^{-6}$ and $\mathcal{B}(D_s^+ \to \phi\pi^+ \to e^+e^-\pi^+) = \mathcal{B}(D_s^+ \to \phi\pi^+) \times \mathcal{B}(\phi \to e^+e^-) = [(4.38 \pm 0.35) \times 10^{-2}] \times [(2.97 \pm 0.04) \times 10^{-4}] = (1.3 \pm 0.1) \times 10^{-5}$.

ACKNOWLEDGMENTS

We gratefully acknowledge the effort of the CESR staff in providing us with excellent luminosity and running conditions. D. Cronin-Hennessy thanks the A.P. Sloan Foundation. This work was supported by the National Science Foundation, the U.S. Department of Energy, the Natural Sciences and Engineering Research Council of Canada, and the U.K. Science and Technology Facilities Council.

---

[1] Q. He *et al.* (CLEO Collaboration), Phys. Rev. Lett. **95**, 221802 (2005).
[2] G. Burdman, E. Golowich, J. Hewett and S. Pakvasa, Phys. Rev. D **66**, 014009 (2002).
[3] S. Fajfer, S. Prelovsek and P. Singer, Phys. Rev. D **64**, 114009 (2001).
[4] S. Fajfer and S. Prelovsek, Phys. Rev. D **73**, 054026 (2006).
[5] S. Fajfer, N. Kosnik and S. Prelovsek, Phys. Rev. D **76**, 074010 (2007).
[6] A. Ali, A. V. Borisov and N. B. Zamorin, Eur. Phys. J. C **21**, 123 (2001).
[7] A. Atre, T. Han, S. Pascoli and B. Zhang, JHEP **0905**, 030 (2009).
[8] R. A. Briere *et al.* (CESR-c and CLEO-c Taskforces, CLEO-c Collaboration), Cornell University, LEPP Report No. CLNS 01/1742 (2001) (unpublished).
[9] Y. Kubota *et al.* (CLEO Collaboration), Nucl. Instrum. Methods Phys. Res., Sect. A **320**, 66 (1992).
[10] D. Peterson *et al.*, Nucl. Instrum. Methods Phys. Res., Sect. A **478**, 142 (2002).
[11] M. Artuso *et al.*, Nucl. Instrum. Methods Phys. Res., Sect. A **502**, 91 (2003).
[12] S. Dobbs *et al.* (CLEO Collaboration), Phys. Rev. D **76**, 112001 (2007).
[13] D. M. Asner *et al.* (CLEO Collaboration), Phys. Rev. D **81**, 052007 (2010).
[14] D. Besson *et al.* (CLEO Collaboration), Phys. Rev. D **80**, 032005 (2009).
[15] R. Brun *et al.*, GEANT 3.21, CERN Program Library Long Writeup W5013 (unpublished) 1993.
[16] D. J. Lange, Nucl. Instrum. Methods Phys. Res., Sect. A **462**, 152 (2001).
[17] E. Barberio and Z. Wąs, Comput. Phys. Commun. **79**, 291 (1994).
[18] C. Amsler *et al.* (Particle Data Group), Phys. Lett. B **667**, 1 (2008).
[19] J. Z. Bai *et al.* (BES Collaboration), Phys. Rev. Lett. **88**, 101802 (2002).
[20] M. Benayoun, S. I. Eidelman, V. N. Ivanchenko and Z. K. Silagadze, Mod. Phys. Lett. A **14**, 2605 (1999).
[21] D. Cronin-Hennessy *et al.* (CLEO Collaboration), Phys. Rev. D **80**, 072001 (2009).
[22] R. M. Barnett *et al.* (Particle Data Group), Phys. Rev. D **54**, 1 (1996).